Support-vector-machine-based sound and vibration signal processing for monitoring milling operations

Wen-Lin Chu[1], Min-Jia Xie[2]

[1]Department of Mechanical Engineering., National Chin-Yi University of Technology
(No.57, Sec. 2, Zhongshan Rd., Taiping Dist., Taichung 41170, Taiwan)
E-mail: wlchu@ncut.edu.tw
[2]Department of Mechanical Engineering., National Chin-Yi University of Technology
(No.57, Sec. 2, Zhongshan Rd., Taiping Dist., Taichung 41170, Taiwan)
E-mail: charlie2302220@gmail.com

To recognize the abnormal state of the CNC milling machine, sound and vibration sensors were set up inside the machine to capture the signals during machining. In this study, the signals are analyzed and labeled with three states: unmachined, machined, and machining chatter. The characteristic values of each state are established by the calculation of approximate entropy for the time domain signals. The model recognition rate can reach up to 95.1% for the states with and without processing and processing flutter.

Key Words : *Machining state detection, approximate entropy, support vector machines*

1. INTRODUCTION

Machine tools have been widely used in today's era, and the future factory will be developed into a 24-hour operation system, gradually becoming a human-free or intelligent chemical factory.[1)] The advantage of this system is not only to increase the output, but also to make the machine replace the manpower, and more importantly, the workers do not need to take care of one or more machines to perform the operation.[2)] Therefore, the machine of the future should be able to detect its own condition and prevent itself in advance under the long time and large amount of operation.[3)] When performing a lot of machining, the tool will wear out and start to be damaged. If the tool continues to be used after a certain period of time, it will cause dynamic cutting errors and machining chatter[4)], which will further affect the quality of the product.

This paper focuses on the machining conditions of CNC milling machines, with reference to industrial-grade sensor microphones or accelerometers that have been used in several papers to perform the study.[5, 6)] Many research papers have extracted signals for algorithmic computation or training of models, Grossi, et al. [7)] obtained the machining signals with a microphone for analysis, and the vibration stability of the spindle can be calculated with only a few signals from cutting tests over a wide range of high speeds. Shi, et al. [8)] The training parameters were deployed by using an ordered-neurons long short-term memory (ON-LSTM) training model and population based training (PBT) with four acceleration gauges on the data set obtained from a large number of milling experiments. The training results are consistent with the spectrum obtained from the original signal by short-time Fourier transform (STFT). In this experiment, the sound and vibration signals are analyzed to compare the difference between the response states of the two signals to processing, and in the signal processing part, Approximate Entropy (ApEn), which has been adopted by many literatures, is used to convert the signals numerically.[9)] Approximate entropy values are often used for analysis and identification of various signals [10, 11)] and are most often used in biomedical-related research. Lahmiri, et al. [12)] By using approximate entropy features, we can effectively distinguish the sound signals of healthy and sick babies' cries. Eventually, a machine learning method, Support Vector Machine (SVM), is used to train a model to identify the processing state.[13)] To avoid the noise of the original signal that causes misjudgment of the training results, this paper uses a finite pulse response filter to eliminate the noise and then conducts model training to increase the recognition of the model training.

2. EXPERIMENTAL EQUIPMENT AND METHODS

To identify the abnormal state of chattering in the milling machine, sound and vibration sensors (microphone and accelerometer) were set up inside the machine to collect the machining signals, and then the signals were analyzed and the state was marked, and finally the identification model was trained. The detailed

specifications of the equipment used in this experiment are summarized in Section 2.1, and the overall experimental structure is described in Section 2.2.

(1) Experimental equipment

The machine equipment used in this experiment is the digital control milling machine (MV154-C) produced by Quaser Machine tools Inc. and the controller is FANUC, as shown in **Fig. 1** The specifications are shown in **Table 1**.

Fig. 1 Digital control milling machine (MV154-C)

Table 1 Digital control milling machine (MV154-C) specification

No.	Specifications	Number of values
1	Workbench size (mm)	900×500
2	X-axis travel(mm)	762
3	Y-axis travel (mm)	530
4	Z-axis travel (mm)	560
5	Spindle nose to workbench distance (mm)	150~710
6	Workbench load (kg)	500
7	Spindle type	Direct-Drive Spindle

The tool used for the experimental machining is a cobalt HSS end mill (H.S.S-Co8 END MILL), as shown in **Fig. 2**.The specifications are shown in **Table 2**. The workpiece material is aluminum alloy (6061), and the workpiece material size is uniformly 100×80×10 mm.

Fig. 2 Cobalt HSS end mill

Table 2 Cobalt HSS end mill specification

No.	Specification	Number of values
1	Blade diameter (mm)	10
2	Shank diameter (mm)	10
3	Blade length (mm)	25
4	Total length(mm)	75
5	Metric three-blade high guide angle	50°

The sound and vibration sensor used in the experiment was a microphone (378B02) made by PCB Piezotronics, which was set up 85 mm from the processing area.[14] Metra Mess-und Frequenztechnik's three-axis accelerometer (KS943B.100) is attached to the side of the spindle.[15] The above equipment is shown in **Fig. 3** to **Fig. 5**, and the specification table is shown in **Table 3** to **Table 5**. The overall experimental equipment setup is shown in **Fig. 6.**

Fig. 3 Microphone (378B02)

Table 3 Microphone (378B02) specification

No.	Specifications	Number of values
1	Sensitivity (mV/Pa)	48.93
2	Frequency Range (±2 dB)(Hz)	3.75~20,000
3	Inherent noise	137 dB re 20 μPa
4	Ambient temperature measurement range (°C)	-40~80
5	Diameter × height (mm)	12.7×90.9
6	Weight (gm)	45.8

Fig. 4 Three-axis acceleration gauge (KS943B.100)

Table 4 Three-axis acceleration gauge (KS943B.100) Specification

No.	Specification	Number of values
1	Sensitivity (mV/g)	100

2	Frequency Range (±3 dB)(Hz)	0.5~22,000
3	Measurement Range(g)	±60
4	Measure the ambient temperature range (℃)	-20~120

Fig. 5 Signal Acquisition Module (NI-9234)

Table 5 Signal Acquisition Module (NI-9234) specification

No.	Specification	Number of values
1	Signal Range(V)	±5
2	Number of channels	4
3	Sampling Frequency (kS/s/ch)	51.2
4	Input Configuration	IEPE
5	Noise at maximum sampling rate (μVrms)	50
6	Connecting Channel	BNC

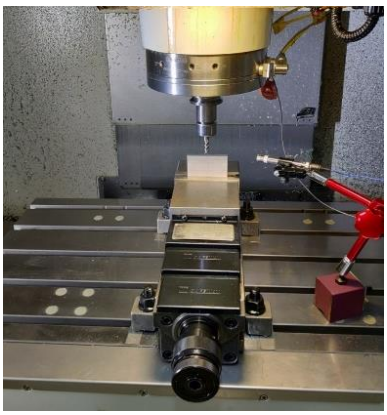

Fig. 6 Experimenting with equipment erection conditions

(2) Experimental Framework

In this study, in order to create a state of tremor during processing, according to Budak and Altintas, [16] Research indicates that the occurrence of chatter is directly related to the two machining parameters of spindle speed and depth of cut. The experimental parameters are shown in **Table 6**. The feed rate is 200 mm/rev, the radial depth of cut is 10 mm, and the machining method is smooth milling. First, the signals of the machining process were collected, and the unmachined environment signals, normal machining signals and machining chatter signals were obtained. After obtaining the signal data, the signal is processed, and the time domain figure is used to classify the processing and unprocessed periods. frequencies (FFT), and based on the period doubling type frequency formula, As shown in equation (1a)[17] the time period between normal processing and tremor processing is classified. The next part of the signal processing is to convert the time domain data of the original signal per second into an Approximate Entropy (ApEn) feature, and finally to build a model to identify the abnormal machining condition by SVM. The detailed process is shown in **Fig. 7**.

$$f_{PD} = \{\frac{z\Omega}{30} + n\frac{\Omega}{60}\}[\text{Hz}], n = ..., -1, 0, 1, ..., \qquad (1a)$$

f_{PD} is chatter frequency; z is the number of flutes in the cutter; Ω is Spindle speed; n is multiplication constant.

Table 6 Experimental processing parameters

Experiment	Spindle speed (r.p.m)	Axial depth of cut (mm)
1	1200	1
2	1200	2
3	1200	4
4	2400	1
5	2400	2
6	2400	4
7	4800	1
8	4800	2
9	4800	4

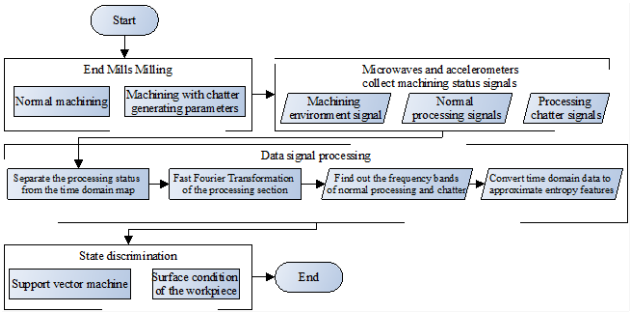

Fig. 7 Experiment Flow Chart

(3) Approximate entropy characteristics

This paper adopts the Approximate Entropy (ApEn) theory proposed by Steve M. Pincus in 1991 for the characterization of numerical conversion.[18]

ApEn is a value that represents the correlation, persistence, or regularity of a Table in a set of time series. The lower the value, the higher the correlation and repetition of the Table's state in this time period; conversely, the higher the ApEn value, the higher the independence and randomness of the Table's state in each second of time series, and the more complex the state. In this paper, we take the processing signal data as an example, and use the

characteristic value of ApEn to distinguish the state of the time domain signal, the data form is shown in equation (2a).

$$x(i) = [u(i), u(i+1), ..., u(i+m-1)], \quad i = 1, 2, ..., (N-m+1) \tag{2a}$$

m is Embed Dimension; N is total amount of data for each calculation; the signal of this experiment is the total number of data points per second, and the Range $1 \le m < N$ of ApEn is defined as shown in equations (3a) to (3d).[19)]

$$\mathrm{ApEn}(m, r, N) = \phi^{m}(r) - \phi^{m+1}(r) \tag{3a}$$

$$\phi^{m}(r) = \frac{1}{N-M+1} \sum_{i=1}^{N-m+1} \log C_i^m(r) \tag{3b}$$

$$C_i^m(r) = \frac{(\text{number of such } j \text{ such that } \mathrm{d}[x(i), \mathrm{x}(j)] \le r)}{(N-M+1)} \tag{3c}$$

$$d[x(i), x(j)] = \max_{k=1,2,...,m}(|u(i+k-1) - u(j+k-1)|) \tag{3d}$$

r is recommended filtering coefficient for noise is 0.1~0.25 times the standard deviation of the total data value within the range.[19, 20)]

(4) Finite impulse response filter

In this paper, it is believed that too much noise in the original signal will easily cause misjudgment in the subsequent model training and lead to poor model stability. Therefore, finite impulse response (FIR Filters) is used for band-pass filtering of the signal. The filtering band ranges from 50 Hz to 5000 Hz, and the lower part of the band is used to remove the signal drift, and the higher part of the band is used to remove the interference of the high frequency noise from the machine[21)], which will make the response before and after the frequency consistent according to the wavelength length of the filter, and the frequency response outside the range is eventually close to zero. Therefore, it is called a limited pulse response filter, and its filter input-output relationship is shown in equation (4a).[22)]

$$\mathrm{y}(n) = \sum_{k=0}^{K} b_k x(n-k) \tag{4a}$$

The output signal response of the filter is y(n) ; input signal is $x(n)$; K the coefficient refers to the order of the filter; the pulse response of the filter is b_k ,also can replace as the filter coefficient.

(5) Support vector machine

In this paper, the final classification of processing states is done by using support vector machines, which are often used in machine learning to classify states. This approach is considered as supervised learning in machine learning in support vector machines, since all states are classified into blocks before the training of the classification model.

The classification method of SVM is to map the training data set to a hyperplane, and to calculate the distance of each data point to each other until we find the maximum distance that can distinguish the two blocks.[23, 24)]

The SVM first calculates the distance in space, the training data consists of points n and is expressed as a vector $(x_i \ d_i)$; x_i is the input vector; d_i is the target value which is the maximum distance, the following equation expresses the target value as 1 and -1, and is mapped to the hyperplane by substituting the target value. The hyperplane distance is expressed as shown in equation (5a).

$$y = \begin{cases} d_i = 1; (w^T x + b) \ge 0 \\ d_i = -1; (w^T x + b) < 0 \end{cases} \tag{5a}$$

y is hyperplane; w is hyperplane weight vector value; x is the vector value of the feature block obtained after mapping the training data set x_i to the hyperplane space; b is the bias of the hyperplane is a constant, which is expressed as shown in equation (6a) by substituting all training data sets.

$$y_i(w^T x + b) \ge 1, i = 1, 2, 3, ..., n \tag{6a}$$

Finally, in order to find the maximum distance (margin) between the two characteristic blocks as shown in Eq. (7a), it is necessary to make the range of the two characteristic blocks as large as possible, and the target function is obtained by substituting Eq. (7b).

$$\text{margin} = \frac{w^T x + b}{\|w\|} \tag{7a}$$

$$\min \frac{1}{2}\|w\|^2 \quad subject\ to \left\{ y_i \left[\left(w^T x_i + b \right) \right] \ge 1, (i = 1, 2, 3, ..., n) \right. \tag{7b}$$

3. EXPERIMENTAL RESULTS

In this paper, the signal interception was carried out for the milling process. The relevant sensors were installed into the machine and the process was carried out according to the experimental parameters in **Table 6**, and the processing signal of the experiment was intercepted. The sampling frequency of the vibration signal collected by the accelerometer was set to 10240 Hz, and the sampling frequency of the sound signal collected by the microphone was set to 25600 Hz.

The time domain signals collected from each sensor are converted into numerical states per second by the approximate entropy feature, and the SVM model is trained by the toolbox in MATLAB R2020a, and the degree of recognition is compared with and without the finite impulse response filter.

(1) Chatter Phenomenon Analysis

In this paper, we determine the occurrence of chattering according to the period doubling type frequencies of Equation (1a). Therefore, the time domain signal of the processing was subjected to Fast Fourier Transform (FFT) to find out the maximum response frequency per second during the processing, and finally the table surface of the workpiece was compared to confirm the occurrence of tremors. First, we observe the time domain figure of all the experiments, and take the time domain figure of experiment 6 to illustrate the signal results as shown in **Fig. 8**.

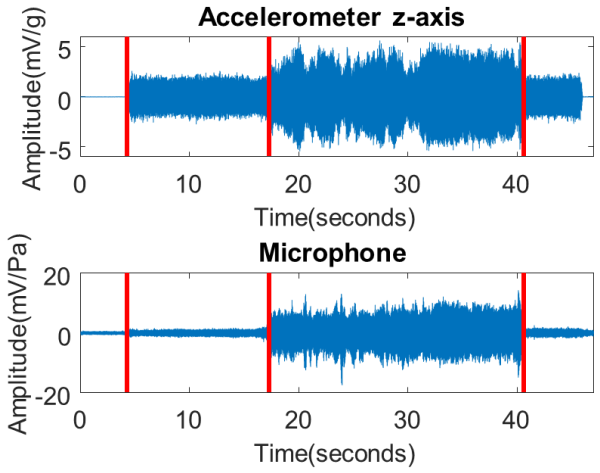

Fig. 8 Processing time domain diagram of Experiment 6

From **Fig. 8**, we can observe the time domain of the whole acquisition process from machine start-up to processing. The first part of the signal is from 0 to 4.3 seconds, which shows that the energy is low and the spindle has not been started yet; the signals from 4.3 to 16 seconds and after 40.6 seconds are the signals from the energy amplitude caused by the spindle rotation between the start of the machine and the end of machining and the spindle stop; and the period from 16 to 40.6 seconds is the signal from the spindle rotation at high speed. In the period from 16 to 40.6 seconds, the energy signal is generated by the high speed rotation of the spindle. The FFT was performed on the processing period from 16 to 40.6 seconds to determine whether the maximum frequency response was close to the frequency value of the frequency multiplier, and to determine whether there was any tremors during the processing period. The results of the conversion of the accelerometer and the microphone signal into frequency are shown in **Table 7** and **Table 8**.

Table 7 Speeding up the frequency of processing periods per second

The maximum frequency response of the Nth second processing period of FFT			
Time(s)	16~17	17~19	19~23
Frequency(Hz)	4574	1314	1316
Time(s)	23~30	30~32	32~36
Frequency(Hz)	1315	1314	1315
Time(s)	36~38	38~40	40~41
Frequency(Hz)	1314	1315	4572

Table 8 Frequency of microphone processing periods per second

The maximum frequency response of the Nth second processing period of FFT			
Time(s)	16~17	17~18	18~19
Frequency(Hz)	3646	2148	1913
Time(s)	19~20	19~20	21~22
Frequency(Hz)	1195	1914	1911
Time(s)	22~23	23~24	24~25
Frequency(Hz)	1195	1913	1912
Time(s)	25~27	27~29	29~30
Frequency(Hz)	1913	1315	2151
Time(s)	30~31	31~32	32~40
Frequency(Hz)	2150	1314	1315
Time(s)	40~41		
Frequency(Hz)	4173		

According to **Table 7** and **Table 8**, the calculated values of Equation (1a) were compared, except for the periods of 16~17 seconds and 40~41 seconds, whose frequencies were not close to the period doubling type frequencies, and the rest of the periods showed tremors. The workpiece after machining is shown in **Fig. 9**.

Fig. 9 Experiment 6 workpiece surface

The surface of the workpiece in **Fig. 9** shows that the machining distance from 16 seconds to 17 seconds is about 3.3(mm), and no tool marks appear on the surface of the workpiece. In view of this, this paper uses equation (1a) and the surface condition of the workpiece to mark the status of the rest of the machining experiments to determine whether chatter occurred.

(2) Finite impulse response filter with approximate entropy theory feature retrieval results

After marking the processing status, this section compares the identification results with and without the use of the filter. First, the original signal classification experiment was conducted, and all the experimental time domain signals were converted to ApEn features with the following parameters: m set to 2; r the coefficients were 0.2 times the standard deviation of the time domain signals per second; N is the total amount of data was the total number of data points of the time domain signals per second. The model recognition results are shown in **Table 9** and **Table 10**.

Table 9 Raw signal with approximate entropy features and SVM classification with or without processed model identification results

	SVM model		
	Linear	Quadratic	Cubic
Recognition	53.7%	61.0%	56.1%
	Fine Gaussian	Medium Gaussian	Coarse Gaussian
Recognition	51.2%	46.3%	53.7%

Table 10 SVM classification of raw signals with and without processing and model identification results of tremor states with approximate entropy features

	SVM model		
	Linear	Quadratic	Cubic
Recognition	46.3%	43.9%	26.8%
	Fine Gaussian	Medium Gaussian	Coarse Gaussian
Recognition	53.7%	48.8%	46.3%

From the SVM model recognition rates obtained in **Table 9** and **Table 10** , it can be observed that the highest recognition rate of the original signal with and without processing was only 61.0%, and the highest recognition rate of the model with and without processing and processing tremor was only 53.7%. Based on the above results, we believe that the original signal has too many noise signals, so the second SVM classification experiment will present the results after filtering the signal.

First, all the experimental raw signals are band-pass filtered at 50~5000 Hz using finite impulse response filter, and then the filtered signals are characterized by ApEn. The results of model recognition are shown in **Table 11** and **Table 12**.

Table 11 Model identification results of the original signal using finite impulse response filter with approximate entropy feature and SVM classification with and without processing state

	SVM model		
	Linear	Quadratic	Cubic
Recognition	87.8%	90.2%	87.8%
	Fine Gaussian	Medium Gaussian	Coarse Gaussian
Recognition	87.8%	87.8%	78.0%

Table 12 The original signal is identified using a finite impulse response filter with an approximate entropy feature to classify the SVM model with or without processing and tremor state

	SVM model		
	Linear	Quadratic	Cubic
Recognition	87.8%	92.7%	63.4%
	Fine Gaussian	Medium Gaussian	Coarse Gaussian
Recognition	95.1%	90.2%	75.6%

The data in **Table 11** and **Table 12** show that after the original signal is filtered with the finite impulse response filter, the SVM classification result is performed by ApEn feature conversion. The recognition rate of the model with or without processing was up to 90.2%, and the recognition rate of the model with or without processing and processing tremor was up to 95.1%, and the recognition rate of each SVM model increased.

4. CONCLUSION

In this paper, we analyze the vibration signals and acoustic signals collected during the machining process to identify the machining time period, and then perform fast Fourier transformations to obtain the maximum response frequency. Then, the signal is converted into ApEn features, and the final result of the classification by SVM achieves 95.1% recognition rate. In order to prevent excessive noise in the original signal, it is necessary to use a finite impulse response filter to bandpass filter the signal.

In the future, we can try different filtering bands to eliminate the remaining frequency intervals that may lead to model misclassification, or adjust the parameters of ApEn so that the processed eigenvalues can make the states of our experiments more obvious and regular, so that the SVM classification results can have a higher recognition rate.

REFERENCES

1) M. M. Mabkhot, A. M. Al-Ahmari, B. Salah, and H. Alkhalefah, "Requirements of the Smart Factory System: A Survey and Perspective," (in English), *Machines,* vol. 6, no. 2, Jun 2018.
2) B. Nie, X. Huang, Y. Chen, A. Li, R. Zhang, and J. Huang, "Experimental study on visual detection for fatigue of fixed-position staff," *Appl Ergon,* vol. 65, pp. 1-11, Nov 2017.
3) W. Liu, C. P. Kong, Q. Niu, J. G. Jiang, and X. H. Zhou, "A method of NC machine tools intelligent monitoring system in smart factories," (in English), *Robotics and Computer-Integrated Manufacturing,* vol. 61, p. 101842, Feb 2020.
4) Z. Y. Wang, Y. S. Yang, Y. Liu, K. Liu, and Y. B. Wu, "Prediction of time-varying chatter stability: effect of tool wear," (in English), *International Journal of Advanced Manufacturing Technology,* vol. 99, no. 9-12, pp. 2705-2716, Dec 2018.
5) M. K. Liu, Y. H. Tseng, and M. Q. Tran, "Tool wear monitoring and prediction based on sound signal," (in English), *International Journal of Advanced Manufacturing Technology,* vol. 103, no. 9-12, pp. 3361-3373, Aug 2019.
6) F. Bleicher, C. M. Ramsauer, R. Oswald, N. Leder, and P. Schoerghofer, "Method for determining edge chipping in milling based on tool holder vibration measurements," (in English), *Cirp Annals-Manufacturing Technology,* vol. 69, no. 1, pp. 101-104, 2020/01/01/ 2020.
7) N. Grossi, F. Montevecchi, L. Sallese, A. Scippa, and G. Campatelli, "Chatter stability prediction for high-speed milling through a novel experimental-analytical approach," (in English), *International Journal of Advanced Manufacturing Technology,* vol. 89, no. 9-12, pp. 2587-2601, Apr 2017.

8) F. Shi, H. R. Cao, Y. K. Wang, B. Y. Feng, and Y. F. Ding, "Chatter detection in high-speed milling processes based on ON-LSTM and PBT," (in English), *International Journal of Advanced Manufacturing Technology,* vol. 111, no. 11-12, pp. 3361-3378, Dec 2020.
9) K. Kecik, K. Ciecielag, and K. Zaleski, "Damage detection by recurrence and entropy methods on the basis of time series measured during composite milling," (in English), *International Journal of Advanced Manufacturing Technology,* vol. 111, no. 1-2, pp. 549-563, Nov 2020.
10) Y. Zhang, J. Li, and J. Wang, "Exploring stability of entropy analysis for signal with different trends," (in English), *Physica a-Statistical Mechanics and Its Applications,* vol. 470, pp. 60-67, Mar 15 2017.
11) S. Nalband, A. Prince, and A. Agrawal, "Entropy-based feature extraction and classification of vibroarthographic signal using complete ensemble empirical mode decomposition with adaptive noise," (in English), *Iet Science Measurement & Technology,* https://doi.org/10.1049/iet-smt.2017.0284 vol. 12, no. 3, pp. 350-359, May 2018.
12) S. Lahmiri, C. Tadj, C. Gargour, and S. Bekiros, "Characterization of infant healthy and pathological cry signals in cepstrum domain based on approximate entropy and correlation dimension," (in English), *Chaos Solitons & Fractals,* vol. 143, p. 110639, Feb 2021.
13) S. F. Ding, Z. B. Zhu, and X. K. Zhang, "An overview on semi-supervised support vector machine," (in English), *Neural Computing & Applications,* vol. 28, no. 5, pp. 969-978, May 2017.
14) R. M. Lee, P. T. Liu, and C. C. Wang, "Investigation of Milling Stability under Cutting Fluid Supply by Microphone Signal Analysis," (in English), *Sensors and Materials,* vol. 30, no. 11, pp. 2419-2428, 2018.
15) C. A. Zhou, K. Guo, Y. Zhao, Z. L. Zan, and J. Sun, "Development and testing of a wireless rotating triaxial vibration measuring tool holder system for milling process," (in English), *Measurement,* vol. 163, p. 108034, Oct 15 2020.
16) E. Budak and Y. Altintas,, "Analytical Prediction of Chatter Stability in Milling—Part II: Application of the General Formulation to Common Milling Systems," *Journal of Dynamic Systems, Measurement, and Control,* vol. 120, no. 1, pp. 31-36, 03/01 1998.
17) T. Insperger, G. Stepan, P. V. Bayly, and B. P. Mann, "Multiple chatter frequencies in milling processes," (in English), *Journal of Sound and Vibration,* vol. 262, no. 2, pp. 333-345, Apr 24 2003.
18) S. M. Pincus and A. L. Goldberger, "Physiological time-series analysis: what does regularity quantify?," (in eng), *Am J Physiol,* vol. 266, no. 4 Pt 2, pp. H1643-56, Apr 1994.
19) A. Delgado-Bonal and A. Marshak, "Approximate Entropy and Sample Entropy: A Comprehensive Tutorial," *Entropy (Basel),* vol. 21, no. 6, May 28 2019.
20) W. L. Chu, M. W. Huang, B. L. Jian, and K. S. Cheng, "Analysis of EEG entropy during visual evocation of emotion in schizophrenia," *Ann Gen Psychiatry,* vol. 16, no. 1, p. 34, 2017/09/25 2017.
21) B. Clauß *et al.*, "Process monitoring and impulse detection in face milling using capacitive acceleration sensors based on MEMS," *Procedia CIRP,* vol. 93, pp. 1454-1459, 2020/01/01/ 2020.
22) L. Yifei and T. Wei, "A Delta Sigma based Finite Impulse Response Filter for EEG Signal Processing," in *2015 IEEE 58th International Midwest Symposium on Circuits and Systems (MWSCAS)*, 2015, pp. 1-4.
23) A. Kothuru, S. P. Nooka, and R. Liu, "Application of audible sound signals for tool wear monitoring using machine learning techniques in end milling," *The International Journal of Advanced Manufacturing Technology,* vol. 95, no. 9, pp. 3797-3808, 2018/04/01 2018.
24) J. Y. Park, Y. G. Yoon, and T. K. Oh, "Prediction of Concrete Strength with P-, S-, R-Wave Velocities by Support Vector Machine (SVM) and Artificial Neural Network (ANN)," *Applied Sciences,* vol. 9, no. 19, 2019.